Acta Crystallographica Section D
Biological Crystallography
ISSN 0907-4449

Structural plasticity in the eight-helix fold of a trematode haemoglobin

Mario Milani,[a] Alessandra Pesce,[a] Sylvia Dewilde,[b] Paolo Ascenzi,[a,c] Luc Moens[b] and Martino Bolognesi[a]*

[a]Department of Physics–INFM, Advanced Biotechnology Centre, University of Genova, Largo Rosanna Benzi 10, I-16146 Genova, Italy, [b]Department of Biochemistry, University of Antwerp, Universiteitsplein 1, B-2610 Antwerp, Belgium, and [c]Department of Biology, University 'Roma Tre', Viale Guglielmo Marconi 446, I-00146 Roma, Italy

Correspondence e-mail: bolognes@fisica.unige.it

Received 13 December 2001
Accepted 31 January 2002

PDB Reference: *P. epiclitum* haemoglobin, 1kfr, r1kfrsf.

The three-dimensional structure of recombinant haemoglobin from the trematode *Paramphistomum epiclitum*, displaying the highest oxygen affinity so far observed for (non)vertebrate haemoglobins, has previously been determined at 1.17 Å resolution (orthorhombic space group $P2_12_12_1$). In the present communication, the three-dimensional structure of wild-type *P. epiclitum* haemoglobin is reported at 1.85 Å resolution in a monoclinic crystal form (R factor = 16.1%, R_{free} = 22.0%). Comparison of *P. epiclitum* (recombinant *versus* wild-type ferric Hb) structures in the two crystal forms shows structural differences in the haem proximal and distal sites which have not been reported for other known haemoglobin structures previously.

1. Introduction

Trematodes are parasites inhabiting various vertebrate body organs, such as the bile duct or stomach of ruminants, where O_2 supply is scarce and intermittent (Kassai, 1999). Trematodes display a set of mono-domain cytoplasmic haemoglobin (Hb) isoforms whose physiological role has been openly debated (Goldberg, 1995; Rashid *et al.*, 1997; Rashid & Weber, 1999). Within the (non)vertebrate globin families, the O_2 affinity for Hb and myoglobin (Mb) varies by several orders of magnitude. This property is achieved through modulation of the O_2 association and dissociation rates resulting from fine structural adaptation of the haem environment both on the porphyrin distal and proximal sides (Bolognesi *et al.*, 1997; Royer *et al.*, 2001). The highest O_2 affinity observed so far in the Hb family is displayed by the trematode *Paramphistomum epiclitum* Hb (PeHb; $P_{50} < 0.1$ Pa; Rashid *et al.*, 1997), which displays some unusual residue substitutions relative to (non)vertebrate Hbs. In particular, Tyr residues are present both at the 32*B*10 and 66*E*7 positions on the haem distal side (Pesce *et al.*, 2001; amino-acid residues are identified by their three-letter code, their sequence number and their topological position within the eight helices of the globin fold; Perutz, 1979).

Recombinant monomeric PeHb has previously been crystallized in our laboratory in the orthorhombic space group $P2_12_12_1$ and the crystal structure has been solved and refined to very high resolution (1.17 Å; Pesce *et al.*, 2001). The recombinant ferric PeHb crystal structure showed that the haem distal site residue Tyr32*B*10 is engaged in hydrogen bonding with the haem-Fe-bound ligand (*i.e.* H_2O molecule w14), whereas Tyr66*E*7 is locked next to the *CD* globin region in a conformation unsuitable for haem ligand stabilization.

Here, we report the crystallographic analysis of a monoclinic crystal form of wild-type ferric PeHb at 1.85 Å resolution. The refined wild-type PeHb structure is compared with that previously reported for the recombinant ferric protein (Pesce *et al.*, 2001), focusing on the functionally relevant distal and proximal haem sides where specific structural differences are observed.

2. Materials and methods

2.1. Crystallization and X-ray data collection of PeHb

P. epiclitum, a parasite of the common Indian water buffalo, was obtained from a slaughterhouse in Aligarh, India. PeHb was purified as previously described (Rashid *et al.*, 1997). Wild-type PeHb was crystallized by vapour-diffusion techniques at a protein concentration of 40 mg ml^{-1} in the presence of potassium ferricyanide. The protein droplet was equilibrated against a reservoir containing 3.0 *M* ammonium sulfate, 50 m*M* sodium acetate pH 5.5 at 277 K. Very thin plate-shaped crystals (~0.020 × 0.020 × 0.005 mm) grew in a few weeks. The crystals were stored in 3.2 *M* ammonium sulfate, 50 m*M* sodium acetate pH 5.5 at 277 K and transferred to the same solution supplemented with 15% glycerol immediately before data collection at 100 K. X-ray diffraction data were collected on the synchrotron beamline X31 (λ = 1.000 Å) at the EMBL Outstation c/o DESY (Hamburg, Germany) to 1.85 Å. Diffraction data were

processed using *DENZO*, *SCALEPACK* (Otwinowski & Minor, 1997) and programs from the *CCP*4 suite (Collaborative Computational Project, Number 4, 1994). The crystals belong to the monoclinic space group $P2_1$ and accommodate one PeHb molecule per asymmetric unit (V_M = 2.2 Å^3 Da^{-1}; 44% solvent content). The crystallographic constants and data-collection statistics are reported in Table 1.

2.2. Structure determination and refinement

The wild-type ferric PeHb structure was solved by molecular-replacement techniques (*EPMR* program; Kissinger *et al.*, 1999), using as search model the structure of recombinant ferric PeHb (PDB code 1h97; Pesce *et al.*, 2001). Structure factors in the 15.0–4.0 Å resolution range were used for both the rotational and translational searches. The highest solution found yielded a correlation coefficient of 58.6 and an *R* factor of 41.0%. After a run of rigid-body refinement and simulated annealing using the program *CNS* (Brünger *et al.*, 1998) at 3.0 Å resolution, the *R* factor and R_{free} values fell to 32.5 and 35.3%, respectively. Restrained crystallographic refinement of coordinates and individual *B* factors, performed with the *REFMAC* program (Murshudov *et al.*, 1999) in the 19.0–1.85 Å resolution range, was alternated with manual model building and water-molecule location using *O* (Jones *et al.*, 1991) and stereochemical considerations.

The refined PeHb model contains 147 amino acids, 180 water molecules and three sulfate ions (*R* factor = 16.1%, R_{free} = 22.0%; see Table 1), with ideal stereochemical parameters (Engh & Huber, 1991). Atomic coordinates and structure factors for wild-type ferric PeHb crystallized in the monoclinic crystal form have been deposited with the Protein Data Bank (Berman *et al.*, 2000).

Table 1
Crystallographic data-collection and refinement statistics of wild-type ferric PeHb.

Outer-shell statistics (1.88–1.85 Å) are shown in parentheses.

PeHb data-collection statistics	
Wavelength (Å)	1.000
Resolution (Å)	19–1.85
Mosaicity (°)	0.66
Completeness (%)	95.9 (94.3)
R_{merge} (%)	10.6
Independent/total reflections	12210/66405
Average $I/\sigma(I)$	9 (3)
Space group	$P2_1$
Unit-cell parameters (Å, °)	a = 41.1, b = 31.4, c = 54.9, β = 95.5
PeHb refinement statistics and model quality	
Resolution range (Å)	19-1.85
Total No. of non-H atoms	1403
No. of water molecules	180
R factor/R_{free}†	0.161/0.220
R.m.s.d. from ideal geometry	
Bond lengths (Å)	0.010
Bond angles (°)	1.12
Ramachandran plot‡	
Most favoured region (%)	95.5
Additional allowed region (%)	4.5
Averaged B factors (Å^2)	
Main chain	11
Side chain	15
Solvent	25

† Calculated using 5% of the reflections. ‡ Data produced using the program *PROCHECK* (Laskowski *et al.*, 1993).

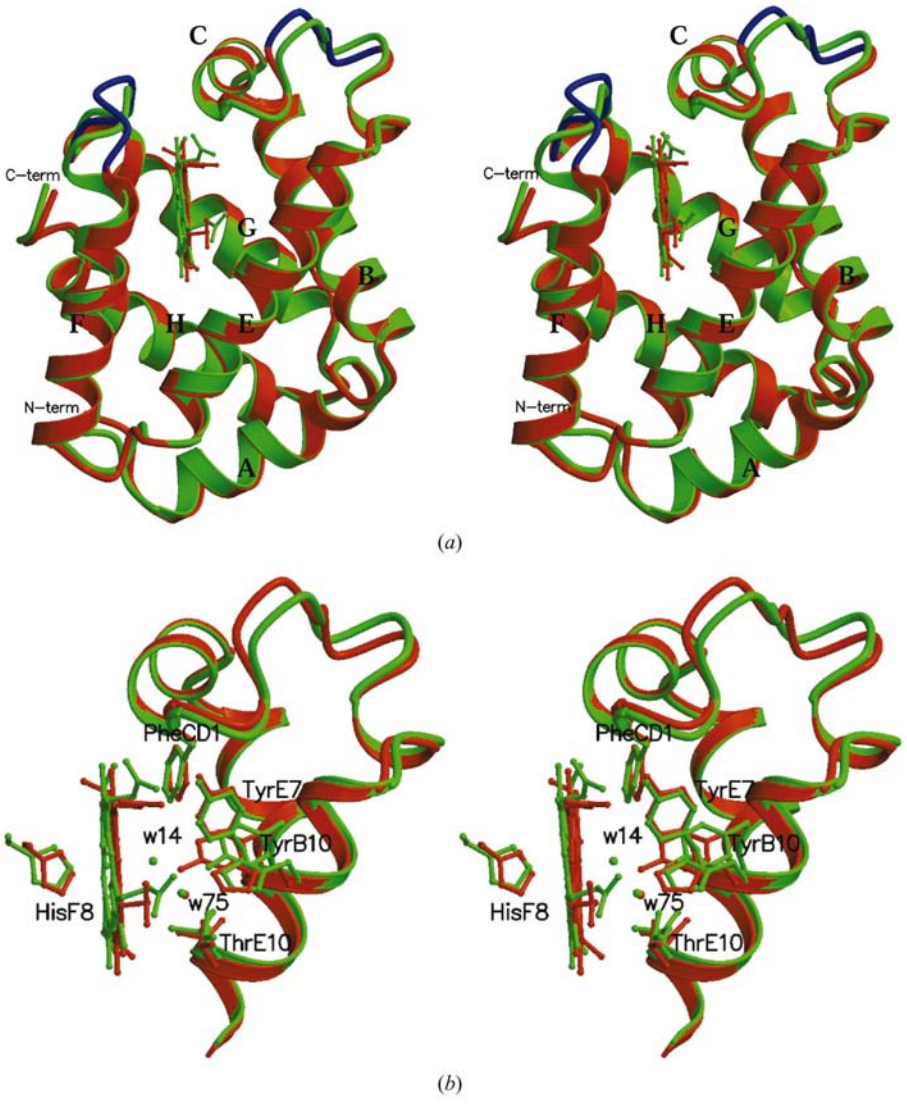

Figure 1
(*a*) Stereoview of the PeHb C$^\alpha$ chains as observed in the orthorhombic recombinant ferric PeHb (green) and monoclinic wild-type ferric PeHb (orange) crystal forms. The *CD–D* (residues 50–55) and *FG* (residues 97–107) regions affected by the largest conformational readjustments are highlighted in blue. (*b*) Structural overlay of orthorhombic recombinant ferric PeHb (green) and monoclinic wild-type ferric PeHb (orange), showing the *CD–D* region, part of the *B* and *E* helices, the main distal and proximal residues and the distal site water molecules w14 and w75. The figures were drawn with *MOLSCRIPT* (Kraulis, 1991).

3. Results and discussion

The two crystal forms of recombinant and wild-type PeHb characterized in our laboratory [space groups $P2_12_12_1$ (Pesce *et al.*, 2001) and $P2_1$ (this study)] were obtained under crystallization conditions differing by one pH unit (pH 4.5 and 5.5, respectively). In particular, the orthorhombic crystals were grown from purified recombinant protein, whereas the monoclinic crystal form was grown from a protein batch isolated from collected trematodes. Wild-type and recombinant PeHbs display indistinguishable O_2-binding properties, although a fraction of recombinant protein molecules bear an additional N-terminal Met residue.

As expected, recombinant and wild-type ferric PeHb display strictly comparable globin structures (r.m.s.d. value of 0.87 Å calculated on 147 C^{α} pairs), with deviations (>1 Å) occurring in the N-terminal region (residues 1–7; C^{α} r.m.s.d. = 1.41 Å), in the *CD–D* region (residues 50–55; C^{α} r.m.s.d. = 1.44 Å) and in the *EF* loop (residues 81–85; C^{α} r.m.s.d. = 1.07 Å). Remarkably, residues 97–107, located between the end of the *F* helix and the beginning of the *G* helix, display the largest C^{α} deviation, with an r.m.s.d. of 2.20 Å (see Fig. 1*a*).

Inspection of the molecular packing within the monoclinic crystal form lattice suggests that the structural perturbations (relative to the orthorhombic PeHb structure) found in the *CD–D* and *FG* regions may be related to intermolecular contacts. In fact, fundamental to the formation of the monoclinic lattice packing is a contact region where mutual interactions between residues His39*C*1, Glu55*D*3 and Arg101*FG*3, each contributed by a different PeHb molecule, are established. Moreover, neighbouring residues in the Glu50*CD*5–Ile54*D*2 and Asp97*F*7–Glu107*G*4 regions are also heavily involved in multiple intermolecular contacts.

On the haem distal side of the monoclinic wild-type ferric PeHb form residues Glu50*CD*5 and Gly51*CD*6 are shifted towards the protein core to avoid clashing with Ala130*H*6 and Ala126*H*2 from a symmetry-related molecule. Moreover, owing to contact with the C-terminal residues (Ala145*H*21–Glu146*H*22) of a symmetry-equivalent molecule, His33*B*11 is shifted by about 0.7 Å, this in turn resulting in a shift of the distal residue Tyr32*B*10 C^{α} toward the haem distal face by 0.74 Å (see Fig. 1*b*). The conformational readjustment at Tyr32*B*10 is further stressed by a side-chain rotation of about 10° such that the Tyr32*B*10 OH—Fe distance drops from 5.53 Å in the orthorhombic crystal form to 3.37 Å in monoclinic PeHb. In agreement with such a short distance between Tyr32*B*10 and the haem, the Fe-coordinated water molecule w14, bound at the sixth coordination position of the haem Fe atom in the orthorhombic recombinant ferric PeHb crystals, is removed in the wild-type monoclinic form. On the other hand, a second water molecule (w75) trapped in the haem distal site of recombinant ferric PeHb (at 4.39 Å from the haem Fe atom) is maintained in wild-type ferric PeHb monoclinic crystals and is strongly hydrogen bonded to Tyr32*B*10 OH (2.75 Å; see Fig. 1*b*).

Within the *FG* loop, residues Ser100*FG*2 and Arg101*FG*3 are those most affected by the monoclinic crystal form packing (C^{α} displacements of 4.09 and 3.41 Å, respectively). Relative to the orthorhombic recombinant ferric PeHb form, Ser100*FG*2 is rotated towards the protein core, to avoid a clash with Gln59*DE*1 from a symmetry-related molecule. On the other hand, residue Arg101*FG*3, which points toward the protein in the orthorhombic crystal form, is extended in the solvent space, establishing an intermolecular salt bridge with His39*C*1 from a nearby PeHb molecule and stabilizing the monoclinic packing. This interaction, as mentioned above, may be pivotal to the achievement of the monoclinic crystal form, since His39*C*1 in turn provides strong hydrogen bonding (2.63 Å) to residue Glu55*D*3 from a symmetry-related molecule. However, the difference in pH values at which the monoclinic and orthorhombic crystal forms grow (pH 5.5 and 4.5, respectively) may only marginally affect the lattice packing at this site. In fact, the calculated overall charge for the His39*C*1 imidazole ring, in the context of the protein structure at the crystallization ionic strength, varies from 0.694 to 0.812 at pH 5.5 and 4.5, respectively (Northrup, 1995).

The structural rearrangements centred around Ser100*FG*2 and Arg101*FG*3 have a direct influence on the overall structure of the haem proximal site of wild-type ferric PeHb. In fact, the proximal His98*F*8 is displaced by 1.62 Å at the C^{α} atom relative to the orthorhombic recombinant ferric PeHb structure (Pesce *et al.*, 2001), displaying a reorientation of the side-chain imidazole ring of about 15° and overall translation of the NE2 atom of 0.54 Å towards the haem. However, since the porphyrin ring is also shifted by about 0.7 Å in the direction of the haem distal cavity, the His98*F*8 NE2—Fe coordination bond is stabilized at 2.13 Å (see Table 2).

As a consequence of crystal packing contacts, the conformational readjustments occurring at the distal and proximal haem sites of wild-type ferric PeHb alter the protein–haem interactions. In particular, residues Ile74*E*15 and Glu107*G*4 provide van der Waals contacts to the porphyrin ring, unique to the wild-type ferric PeHb monoclinic form, while protein–haem contacts established in the orthorhombic recombinant ferric PeHb form by residues Tyr42*C*4, His45*C*7, Arg101*FG*3 and the hydrogen bonds between Ser47*CD*2 (N and OG atoms) and the haem propionates, are lost in the monoclinic wild-type ferric PeHb structure. Interestingly, key distal residues, particularly Tyr66*E*7, Thr69*E*10 and Leu79*E*11, and water molecule w75 trapped in the distal cavity but not bound to the haem Fe, are little affected by the haem-pocket conformational readjustments observed in the wild-type ferric PeHb monoclinic crystals (see Fig. 1).

Table 2
Coordination geometry at the ferric haem Fe centres of recombinant and wild-type ferric PeHb.

Coordination bond (Å)	Recombinant PeHb† orthorhombic crystals		Wild-type PeHb‡ monoclinic crystals
	Chain *A*	Chain *B*	
Average Fe—N (pyrrole)	2.01	2.01	2.03
His*F*8 NE2—Fe	2.03	2.02	2.13
Fe—O (ligand)	2.55	2.56	—
Fe—haem plane deviation (Å)	−0.004	−0.016	−0.040
Tilt angle§ (°)	3.9	3.8	5.5
Dihedral NA—Fe—NE2—CE1 (°)	44.9	47.0	42.2

† From Pesce *et al.* (2001). ‡ Present study. § The tilt angle lies between the line Fe—His98*F*8 NE2 and the normal to the mean haem plane.

4. Conclusions

The crystallographic analysis of wild-type ferric PeHb in a monoclinic crystal form sheds insight on the influence of two unrelated crystal packing environments on the structural properties of a monomeric Hb. To our knowledge, this is the first case reported within monomeric members of the Hb superfamily where localized but significant structural perturbations ascribed to crystal packing contacts are observed. Although the orthorhombic and monoclinic PeHb crystal forms were obtained using different protein batches (*i.e.* recombinant PeHb purified from *Escherichia coli* cultures and protein purified from adult trematode *P. epiclitum*), biochemical characterization of the protein samples (see Pesce *et al.*, 2001) and analysis of crystal packing do not suggest any functional or structural influence of the additional N-terminal Met residue present in the recombinant protein.

The crystallographic analysis of monoclinic wild-type ferric PeHb shows localized conformational perturbations within the globin fold, so far held to represent a rather rigid α-helical structure. Such an observation may bear functional implications, since the conformational readjustments observed at the wild-type ferric PeHb haem distal and proximal sites, affecting the coordination and stereochemistry of the haem, suggest an unprecedented structural plasticity of the haem pocket and of the O_2-binding site. In this context, the PeHb residue Tyr66*E*7 had

previously been proposed to stabilize the haem-Fe-bound distal ligand through hydrogen bonding, based on NMR and modelling considerations (Zhang *et al.*, 1997). The 1.17 Å recombinant ferric PeHb structure (orthorhombic crystal form) showed, on the other hand, that Tyr66*E*7 is held in an open conformation by loose hydrogen bonding to Arg48*CD*3 N, Ser47*CD*2 N and OG, as well as by van der Waals contacts with Phe46*CD*1, Leu49*CD*4 and His65*E*6. As a result, the Tyr66*E*7 OH group was located 9.16 Å from the haem Fe atom in the protein *CD* region. On this basis, Pesce *et al.* (2001) argued that conformational transitions of several intervening residues in the haem distal site would be required to allow the shift of the Tyr66*E*7 side chain into the haem distal pocket for effective ligand stabilization. The present results show that, despite the unexpected globin-fold plasticity and the ensuing conformational changes observed at the PeHb haem distal/proximal sites and *CD*–*D* region, the open conformation of Tyr66*E*7 is scarcely affected, leaving residue Tyr32*B*10 as the most likely candidate for stabilization of the haem-Fe-bonded O_2 by hydrogen bonding.

This work was supported by grants from the Italian Space Agency (I/R/167/01) and from the Italian Ministry of University and Research (L95/95). SD is a postdoctoral fellow of the FWO (Fund for Scientific Research). The Fund is also acknowledged for grants to LM (project No. 3G031400). Access to the EMBL Hamburg Outstation was supported by a grant from the EU programme 'Improving the Human Research Potential and Socio-Economic Knowledge Base', subprogram 'Access to Research Infrastructures' (contract number: HPRI-CT-1999-00017).

References

Bolognesi, M., Bordo, D., Rizzi, M., Tarricone, C. & Ascenzi, P. (1997). *Prog. Biophys. Mol. Biol.* **68**, 29–68.

Berman, H. M., Westbrook, J., Feng, Z., Gilliland, G., Bhat, T. N., Weissig, H., Shindyalov, I. N. & Bourne, P. E. (2000). *Nucleic Acids Res.* **28**, 235–242.

Brünger, A. T., Adams, P. D., Clore, G. M., Delano, W. L., Gros, P., Grosse-Kunstleve, R. W., Jiang, J.-S., Kuszewski, J., Nilges, M., Pannu, N. S., Read, R. J., Rice, L. M., Simonson, T. & Warren, G. L. (1998). *Acta Cryst.* D**54**, 905–921.

Collaborative Computational Project, Number 4 (1994). *Acta Cryst.* D**50**, 760–763.

Engh, R. A. & Huber, R. (1991). *Acta Cryst.* A**47**, 392–400.

Goldberg, D. E. (1995). *Bioessays*, **17**, 177–182.

Jones, T. A., Zou, J. Y., Cowan, S. W. & Kjeldgaard, M. (1991). *Acta Cryst.* A**47**, 110–119.

Kassai, T. (1999). *Veterinary Helminthology*. Oxford: Butterworth & Heinemann.

Kissinger, C. R., Gehlhaar, D. K. & Fogel, D. B. (1999). *Acta Cryst.* D**55**, 484–491.

Kraulis, P. J. (1991). *J. Appl. Cryst.* **24**, 946–950.

Laskowski, R. A., MacArthur, M. W., Moss, D. S. & Thornton, J. M. (1993). *J. Appl. Cryst.* **26**, 283–291.

Murshudov, G. N., Lebedev, A., Vagin, A. A., Wilson, K. S. & Dodson, E. J. (1999). *Acta Cryst.* D**55**, 247–255.

Northrup, S. H. (1995). *MacroDox* v.2.0.2. *Software for the Prediction of Macromolecular Interaction.* Tennessee Technological University, Cookeville, TN, USA.

Otwinowski, Z. & Minor, W. (1997). *Methods Enzymol.* **276**, 307–326.

Perutz, M. F. (1979). *Annu. Rev. Biochem.* **48**, 327–386.

Pesce, A., Dewilde, S., Kiger, L., Milani, M., Ascenzi, P., Marden, M. C., Van Hauwaert, M. L., Vanfleteren, J., Moens, L. & Bolognesi, M. (2001). *J. Mol. Biol.* **309**, 1156–1164.

Rashid, A. K., Van Hauwaert, M. L., Haque, M., Siddiqi, A. H., Lasters, I., De Maeyer, M., Griffon, N., Marden, M. C., Dewilde, S., Clauwaert, J., Vinogradov, S. N. & Moens, L. (1997). *J. Biol. Chem.* **272**, 2992–2999.

Rashid, A. K. & Weber, R. E. (1999). *Eur. J. Biochem.* **260**, 717–725.

Royer, W. E. Jr, Knapp, J. E., Strand, K. & Heaslet, H. A. (2001). *Trends Biochem. Sci.* **26**, 297–304.

Zhang, W., Rashid, K. A., Haque, M., Siddiqi, A. H., Vinogradov, S. N., Moens, L. & La Mar, G. N. (1997). *J. Biol. Chem.* **272**, 3000–3006.